Synthesis of PdAu/C and PdAuBi/C Electrocatalysts by Borohydride Reduction Method for Ethylene Glycol Electro-oxidation in Alkaline Medium

Michele Brandalise[1], Marcelo Marques Tusi[2], Ricardo Marcelo Piasentin[1],
Mauro Coelho dos Santos[3], Estevam Vitorio Spinacé[1], Almir Oliveira Neto[1,]*

[1] Instituto de Pesquisas Energéticas e Nucleares – IPEN/CNEN-SP, Av. Prof. Lineu Prestes, 2422 – Cidade Universitária – CEP 05508-900 São Paulo, SP, Brazil.
[2] Universidade Regional Integrada do Alto Uruguai e das Missões – URI, Av. Batista Bonoto Sobrinho, s/n – São Vicente – CEP 97700-000 Santiago, RS, Brazil.
[3] Universidade Federal do ABC – UFABC, R. Santa Adélia, 166 – Bangu – CEP 09210-170 Santo André, SP, Brazil.
[*]E-mail: aolivei@ipen.br

Pd/C, Au/C, AuBi/C, PdAu/C, PdAuBi/C electrocatalysts (with different atomic ratios and 20 wt% of metal loading) were prepared by borohydride reduction method using a water/2-propanol mixture as solvent, $Pd(NO_3)_2.2H_2O$, $HAuCl_4.3H_2O$ and $Bi(NO_3)_3.5H_2O$ as metal sources, carbon black Vulcan XC72 as support and $NaBH_4$ as reducing agent. The obtained electrocatalysts were characterized by energy dispersive X-ray analysis (EDX), X-ray diffraction (XRD), transmission electron microscopy (TEM) and cyclic voltammetry. The activities of the prepared electrocatalysts for ethylene glycol electro-oxidation were investigated by chronoamperometry using the thin porous coating technique. The atomic ratios of the electrocatalysts determined by EDX were similar to the nominal values. The X-ray diffratograms of Pd/C and PdAu/C showed the presence of Pd(fcc) phase and Pd-Au(fcc) alloys, respectively. Depending on the Au content, segregated fcc Pd-rich and Au-rich phases were observed in the PdAu/C electrocatalysts. PdAuBi/C also showed the presence of fcc alloys while for Bi/C the presence of bismuth oxide phase was observed. TEM micrographs of all electrocatalysts showed a mean particle sizes in the range of 5–8 nm and a monomodal and relatively broad distribution of particle sizes. Electrochemical experiments indicate that the PdAuBi/C (50:45:05) electrocatalyst has the higher electroactivity than others obtained electrocatalysts.
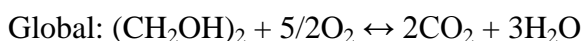
1. INTRODUCTION

Fuel cells are electrochemical devices that convert chemical energy directly into electrical energy with high efficiency and low or none pollutant emission [1-4]. The use of hydrogen as a fuel allows to reach higher current densities; however hydrogen still presents problems of production, storage, and delivery [2,5-8]. Thus, the use of alcohols as a fuel has been considering very promising and direct alcohol fuel cells (DAFC) are considering very attractive as power sources for stationary, mobile and portable applications [9-13]. In DAFCs, the alcohol is feed without any previous chemistry modification or purification and it is oxidized at the anode wile oxygen (usually from air) is reduced at the cathode. The direct feeding of alcohol, allied with the fact that alcohols are liquid at room temperature and they have a well-development infrastructure for production, storage and delivery, avoids similar problems to those associated with the hydrogen [10,12,14].

Most part of studies about electrocatalysis applied in fuel cell science is in acidic medium and Pt-based electrocatalysts have the higher activity in this medium [15,16]. Recently, an increase in the interest about electrocatalysis in alkaline medium has been observed. This increase has been motivated by the advances in the development of anion exchange membranes for application in fuel cells directly fed with liquid fuels [14,16-18]. Compared to acidic DAFCs, the alkaline direct alcohol fuel cells (ADAFC) present the follow advantages: (i) The flow of the charge transport from cathode to anode avoids the crossover of alcohol provide from anode to cathode; (ii) the kinetics of alcohol oxidation and oxygen reduction reactions in alkaline medium are faster than in acidic medium; (iii) the fuel cell components practically do not corrode, consequently, low costs materials can be used and a potential greater longevity can be observed; (iv) it allows the use of Pt-free electrocatalysts [14,19].

Ethylene glycol has been tested as a fuel in ADAFCs due its ease of transport, favorable storage, low vapor pressure, non-toxic nature and ready availability [14,20-24]. The ethylene glycol has a power density of 5.2 $kWhKg^{-1}$, comparable value to the power density of methanol (6.1 $kWhKg^{-1}$) and ethanol (8.6 $kWhKg^{-1}$) [21]. The complete electro-oxidation of ethylene glycol to CO_2 produces 10 electrons per molecule [21,24,25]. An alkaline direct ethylene glycol fuel cell (ADEGFC) that oxidizes completely the ethylene glycol presents the follow reactions [25]:

Anode: $(CH_2OH)_2 + 10OH^- \leftrightarrow 2CO_2 + 8 H_2O + 10e^-$
Cathode: $5/2O_2 + 5H_2O + 10e^- \leftrightarrow 10OH^-$
Global: $(CH_2OH)_2 + 5/2O_2 \leftrightarrow 2CO_2 + 3H_2O$

However, the electro-oxidation of the ethylene glycol to CO_2 in alkaline medium continues to be a challenge and oxalate, glyoxylate, glycolate, glycolaldehyde and glyoxal are the principal products formed [26-28].

As mentioned, Pt and Pt-based materials have been extensively used as the electrocatalysts for the electro-oxidation of liquid fuels such as methanol, ethanol and ethylene glycol in acidic and alkaline medium. However, the high price and limited supply of Pt constitute a barrier to the development of DAFCs [14]. Studies on the development of Pt-free electrocatalysts for alcohol oxidation have revealed that Pd is a good electrocatalyst for alcohol electro-oxidation in alkaline

medium. It was reported that Pd/C showed an electrocatalytic activity higher than that of Pt/C, the onset potential for ethanol oxidation on Pd/C also was shifted to lower potentials compared to that of Pt in alkaline medium and the Pd/C electrocatalysts also shown high stability for alcohol electro-oxidation in alkaline medium [29,30]. Pd-based electrocatalysts are attractive because Pd is at least fifty times more abundant than Pt [31,32]. However, the price of Pd is relatively expensive and therefore Pd loading must be decreased. One effective approach to cost reduction is to reduce the usage of the Pt and Pd catalysts by addition of other metals such as Au [33,34] and Bi [16,17].

Gold (Au) is a metal of the platinum group and it is more abundant and cheaper than Pt and Pd therefore it is a promising alternative to application as electrocatalysts for fuel cells [33,34]. Gold is generally considered as a poor electrocatalyst in acid medium, but its activity in alkaline medium is enhanced [35]. The reactivity of ethanol on Au in alkaline medium is related to the fact that practically no poisoning species (CO-like species) can be formed and adsorbed on the surface [35,36]. Choi *et al*. [37] found that PtAu/C electrocatalysts have enhanced activity for methanol electro-oxidation compared to Pt/C electrocatalysts. Jin *et al* [24] showed that PtAu/C electrocatalysts have high activity and stability in alkaline solution for ethylene glycol oxidation. Su *et al* [38] showed that the addition of Au to Pd/C significantly promotes the catalytic activity and poisoning tolerance of Pd electrocatalysts for ethanol and isopropanol electro-oxidation in alkaline medium.

Some studies reported the benefic effect of the addition of bismuth to Pt-based [17,21,39] and Pd-based [16] electrocatalysts. Demarconnay *et al* [21] showed that PtBi/C electrocatalysts promoted the catalytic activity towards ethylene glycol electro-oxidation in alkaline medium when compared to Pt/C. Riviera *et al* [39] reported that the promotion of Bi on the PtBi catalysts was ascribed to a combination of the ensemble and electronic effects, though Demarconnay *et al* [21] have been considered the Bi action was due bifunctional activity of hydroxylated Bi species. Tusi *et al* [17] reported that the activity of PtBi/C electrocatalysts for ethanol electro-oxidation in alkaline medium increases with Bi content and it could be related to enhancement of OH species absorption on Pt sites adjacent to Bi, which facilitates the oxidative removal of intermediates formed. Neto *et al* [16] showed that the addition of small quantities of Bi (5 at.%) to Pd/C electrocatalyst greatly enhanced the performance for ethanol electro-oxidation in alkaline medium.

Thus, in this work Pd/C, Au/C, AuBi/C (80:20), AuBi/C (95:05), PdAu/C (50:50), PdAu/C (80:20), PdAu/C (95:05), PdAuBi/C (50:45:05), PdAuBi/C (80:10:10) and PdAuBi/C (90:05:05) electrocatalysts were prepared by borohydride reduction method and characterized by energy dispersive X-ray analysis (EDX), X-ray diffraction (XRD), transmission electron microscopy (TEM) and cyclic voltammetry. The obtained electrocatalysts were tested for ethylene glycol electro-oxidation in alkaline medium by chronoamperometry using the thin porous coating technique.

2. EXPERIMENTAL

Pd/C, Au/C, AuBi/C (80:20), AuBi/C (95:05), PdAu/C (50:50), PdAu/C (80:20), PdAu/C (95:05), PdAuBi/C (50:45:05), PdAuBi/C (80:10:10) and PdAuBi/C (90:05:05) electrocatalysts with (20 wt% of metal loading) were prepared by borohydride reduction method [40-42] using

HAuCl$_4$.3H$_2$O Pd(NO$_3$)$_2$.2H$_2$O (Aldrich), HAuCl$_4$.3H$_2$O (Aldrich) and Bi(NO$_3$)$_3$.5H$_2$O (Aldrich) as metal sources and carbon black Vulcan XC72 (Cabot) as support material. The metal sources were dissolved in a mixture of water/2-propanol (50/50, v/v) and the carbon support was dispersed in the solution. The resulting mixture was submitted to an ultrasonic bath for 5 min. After this a solution of sodium borohydride was added under stirring in one portion at room temperature. Finally, the obtained solid was filtered, washed with water and dried at 70 ºC for 2 h. The preparation of electrocatalysts was realized in accordance with reference 16 and 17.

The atomic ratios of the electrocatalysts were obtained by EDX analysis using a scanning electron microscope Phillips XL30 with a 20 keV electron beam and equipped with EDAX DX-4 microanaliser.

X-ray diffraction (XRD) analyses were performed using a Rigaku diffractometer model Miniflex II using Cu Kα radiation source (l = 0.15406 nm). The diffractograms were recorded from 2θ = 20° to 90° with a step size of 0.05° and a scan time of 2 s per step.

Transmission electron microscopy (TEM) was carried out using a JEOL JEM-2100 electron microscope operated at 200 kV. The particle size distributions were determined by measuring 200 nanoparticles from micrographs using an Image Tool Software.

Electrochemical studies of electrocatalysts were carried out using the thin porous coating technique [43,44]. An amount of 20 mg of the electrocatalyst was added to a solution of 50 mL of water containing 3 drops of a 6% solution polytetrafluoroethylene (PTFE) suspension. The resulting mixture was treated in an ultrasound bath for 10 min, filtered and transferred to the cavity (0.30 mm deep and 0.47 cm2 area) of the working electrode. In cyclic voltammetry and chronoamperommetry experiments the current values (I) were expressed in amperes and were normalized per gram of platinum (A gPt^{-1}). The quantity of platinum was calculated considering the mass of the electrocatalyst present in the working electrode multiplied by its percentage of platinum. The reference electrode was an Ag/AgCl electrode and the counter electrode was a Pt plate.

Cyclic voltammetry experiments were performed in 1.0 mol L^{-1} KOH solution saturated with N$_2$ using an AutoLab PGSTAT 30 potentiostat/galvanostat in presence and absence of 1.0 mol L^{-1} of ethylele glycol, while that the chronoamperommetry curves of the ethylene glycol electro-oxidation on obtained electrocatalysts were performed holding the cell potential at −0.4 V vs Ag/AgCl electrode (0.5 V vs RHE) in 1.0 mol L^{-1} KOH solution containing 1.0 mol L^{-1} of ethylene glycol at room temperature.

3. RESULTS AND DISCUTION

Table 1 shows the results of EDX analysis and average crystallite size calculated by Scherrer equation for the prepared electrocatalysts. EDX analysis showed that all obtained electrocatalysts have atomic ratios similar to the nominal values.

Table 1. Atomic ratios and average crystallite sizes of the Pd/C, Au/C, AuBi/C, PdAu/C and PdAuBi/C electrocatalysts.

electrocatalyst	atomic ratio (nominal)	atomic ratio (EDX)	Average crystallite size (nm)
Pd/C	-	-	2
Au/C	-	-	12
AuBi/C	80:20	76:24	8
AuBi/C	95:05	94:06	7
PdAu/C	50:50	55:45	7
PdAu/C	80:20	80:20	2
PdAu/C	95:05	95:05	2
PdAuBi/C	50:45:05	56:39:05	6
PdAuBi/C	80:10:10	79:11:10	2
PdAuBi/C	90:05:05	93:04:03	2

Figure 1 presents the X-ray diffractograms of binaries (Fig. 1a) and ternaries (Fig. 1b) electrocatalysts. The division of data in two graphics was made to provide a clear visualization. All obtained electrocatalysts showed a broad peak at about $2\theta = 25°$ associated to the carbon support material. The Pd/C, PdAu/C and PdAuBi/C electrocatalysts presented five peaks at about $2\theta = 40°$, $47°$, $68°$, $82°$ and $87°$ associated, respectively, to (111), (200), (220), (311) and (222) planes of face-centered cubic (fcc) structure of Pd and Pd alloys [16,45,46]. PdAu/C (50:50), PdAu/C (80:20) and PdAu/C (95:05) electrocatalysts presents a shift to smaller angles of the peak associated to the (220) plane of Pd phase compared to Pd/C electrocatalyst indicating the insertion of Au in the Pd structure.
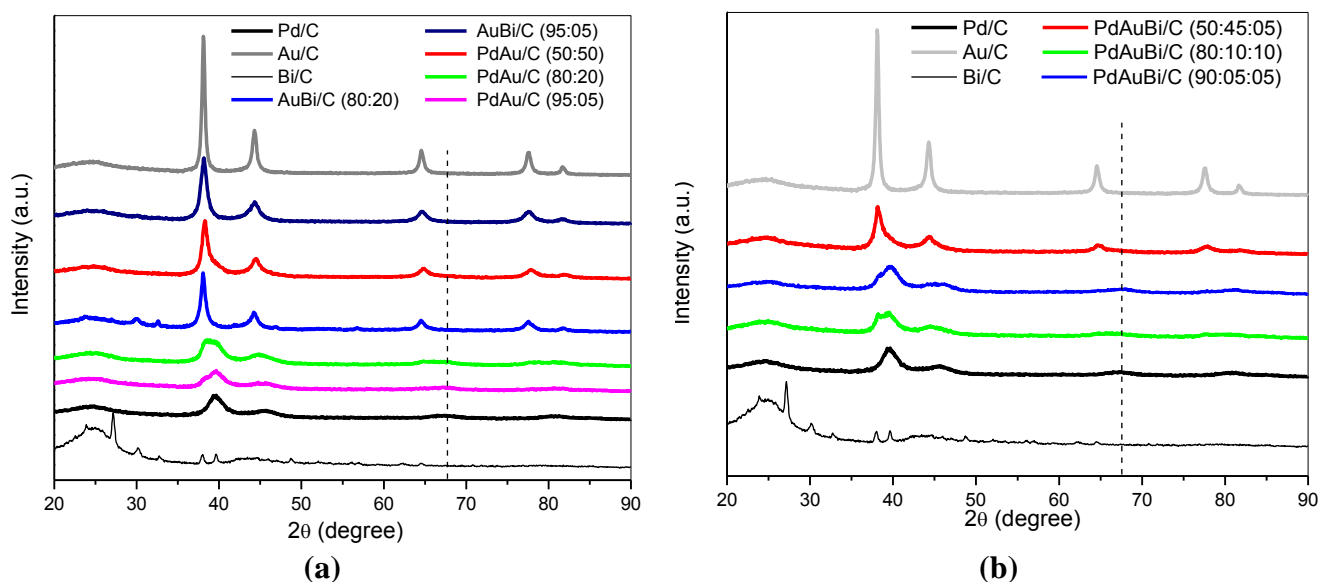
Figure 1. X-ray diffractograms of **(a)** binary and **(b)** ternary electrocatalysts. Both figures have the diffractograms of Pd/C, Au/C and Bi/C to comparative aims.

However, depending on the Au content (low content), segregated fcc Pd-rich and Au-rich phases were observed for PdAu/C electrocatalysts. In the case of PdAuBi/C electrocatalysts the shift of

the peak of Pd(111) can be associated to insertion of Au and Bi in the Pd fcc structure. For PdAuBi/C, depending on the Au content (low content) segregated phases of Pd and Au were also observed as related in previous work [47-50]. Bi/C electrocatalyst presents peaks at about $2\theta = 27°$, $30°$, $38°$, $39°$, $49°$, $52°$, $57°$, $62°$, $64°$ and $70°$ ascribed to bismuth oxide phase (Bi_2O_3) [51,52]. The AuBi/C electrocatalysts show peaks at about $2\theta = 38°$, $44°$, $65°$ and $78°$ associated, respectively, to (111), (200), (220) and (311) planes of fcc structure of Au [53,54]. AuBi/C (80:20) electrocatalyst also showed peaks at about $2\theta = 29°$, $33°$ e $57°$ associated to bismuth oxide phase (Bi_2O_3) [51,52,55-57]. Others electrocatalysts containing bismuth show no peaks associated to the bismuth oxides phases, however their presence could not be discarded.

The average crystallite sizes of Pd/C, PdAu/C and PdAuBi/C electrocatalysts (calculated by Scherrer equation) [58] considering the peak of (220) plane of the Pd (fcc) structure were in the range of 2 to 7 nm. The average crystallite sizes of Au/C and AuBi/C calculated considering the peak of (220) plane of the Au(fcc) structure were in the range of 7 to 12 nm. Therefore the average crystallite sizes increase with the increase of Au content.

TEM micrographs and histograms of the particle size distributions of Pd/C, Au/C, PdAu/C (50:50), PdAu/C, PdAuBi/C (50:45:05) and PdAuBi/C (90:05:05) electrocatalysts are shown in Figure 2. All images showed that the nanoparticles where not well dispersed on the carbon support and some agglomerates were present. It was also observed a monomodal and relatively broad distribution of particle sizes for all electrocatalysts.

The mean particle sizes of Pd/C, Au/C, PdAu/C (95:05) and PdAu/C (50:50) electrocatalysts were 5 nm, 6 nm, 6 nm and 8 nm, repectively. Then, the increase of Au content in PdAu/C electrocatalysts resulted in an increase of mean particle size. Probably this could be explained in the following manner: Au is more noble than Pd and reduces forming Au seeds with Pd growing epitaxially on its surface rather than forming a new nucleus [59].

(a)   (b)   (c)
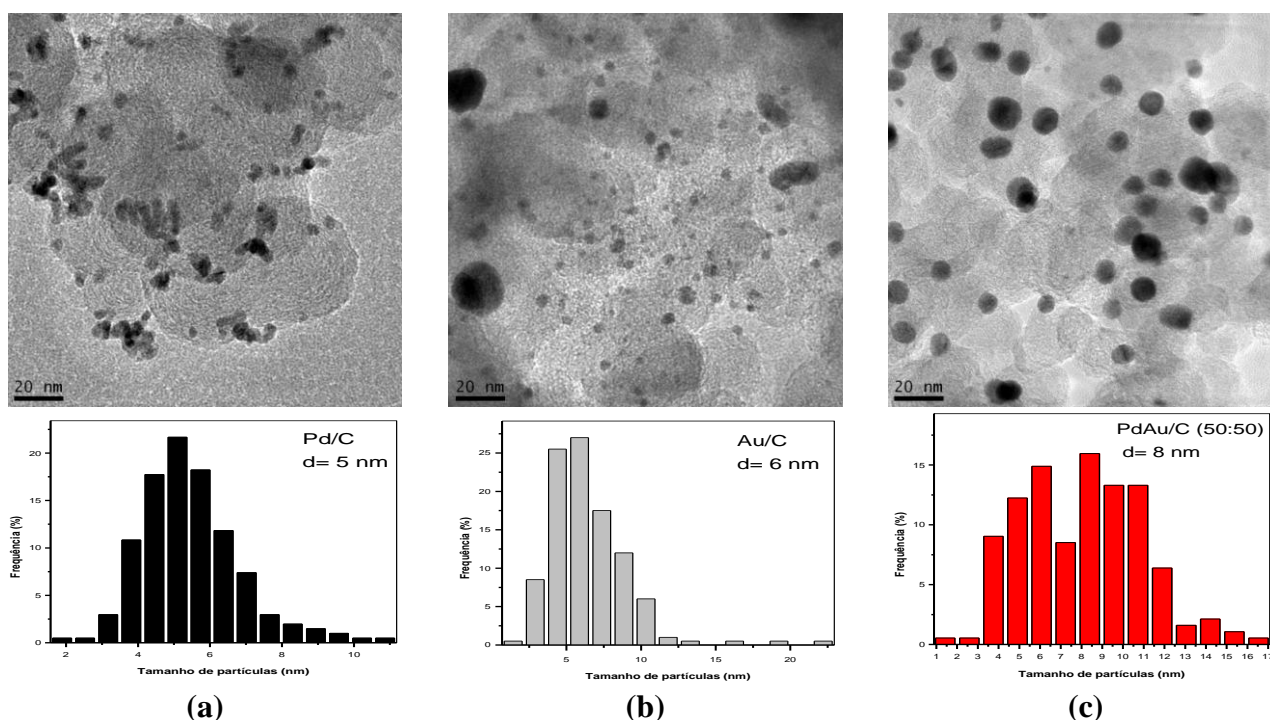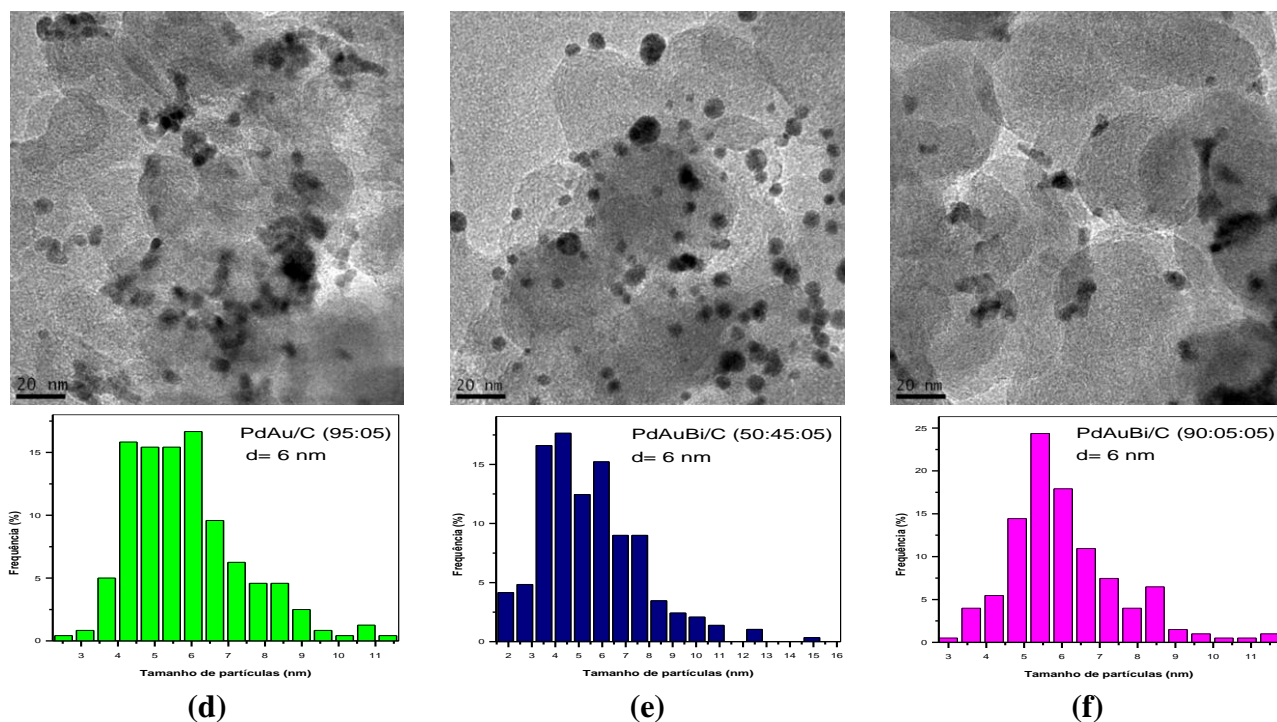
Figure 2. TEM micrographs and histograms of the particle size distribution of (a) Pd/C, (b) Au/C, (c) PdAu/C (50:50), (d) PdAu/C (95:05), (e) PdAuBi/C (50:45:05) and (f) PdAuBi/C (90:05:05).

This phenomenon was observed by Zhu *et al* [59] in the two-step synthesis of Pd@Au/C electrocatalysts from nano-Au seeds (previously prepared by $AuCl_4^-$ reduction in the first step) and posterior reduction of H_2PdCl_4 in the second step. The PdAuBi/C (50:45:05) and PdAuBi/C (90:05:05) electrocatalysts showed a mean particle size of 6 nm.

The cyclic voltammograms of Au/C, Bi/C and AuBi/C electrocatalysts in 1.0 mol L^{-1} KOH solution are shown in Figure 3. All electrocatalysts do not have an well-defined hydrogen adsorption-desorption region (-0.85 to -0.45 V *vs* Ag/AgCl). This data indicated that hydrogen adsorption process does not happen on gold or bismuth [60]. In the range of potentials studied, the AuBi/C electrocatalysts presented various peaks associated to different oxidation states of Bi. The peak observed around -0.45 V and above relates to oxidation of bismuth metal through a reaction mechanism including the formation of bismuth(I) which through disproportionation generates Bi(III) and metallic Bi. Bismuth(III) reacts further with OH$^-$ ions and generates Bi(OH)$_3$. The peak observed at about -0.60 V corresponds analogously to oxidations of metallic Bi [60,61]. As observed, this peak increases both with the amount of Bi added reflecting that an increasing amount of Bi was released and redeposited on the electrode surface during the scan procedure. In the cathodic direction the main peak appears at about -0.70 V and it was associated to the reduction of dissolved BiO$_2^-$ [60].

Figure 4 presents the cyclic voltammograms of Pd/C, Au/C and PdAu/C electrocatalysts in 1.0 mol L^{-1} KOH solution. The Pd/C, PdAu/C (50:50), PdAu/C (80:20) and PdAu/C (95:05) electrocatalysts showed a well-defined hydrogen adsorption-desorption region (peaks in the range of -0.85 to -0.45 V *vs* Ag/AgCl) [62-64]. Thus, the hydrogen adsorption occurs on Pd surface, however

such process did not occur on Au surface once that the hydrogen adsorption-desorption region is suppressed in Au/C electrocatalyst.
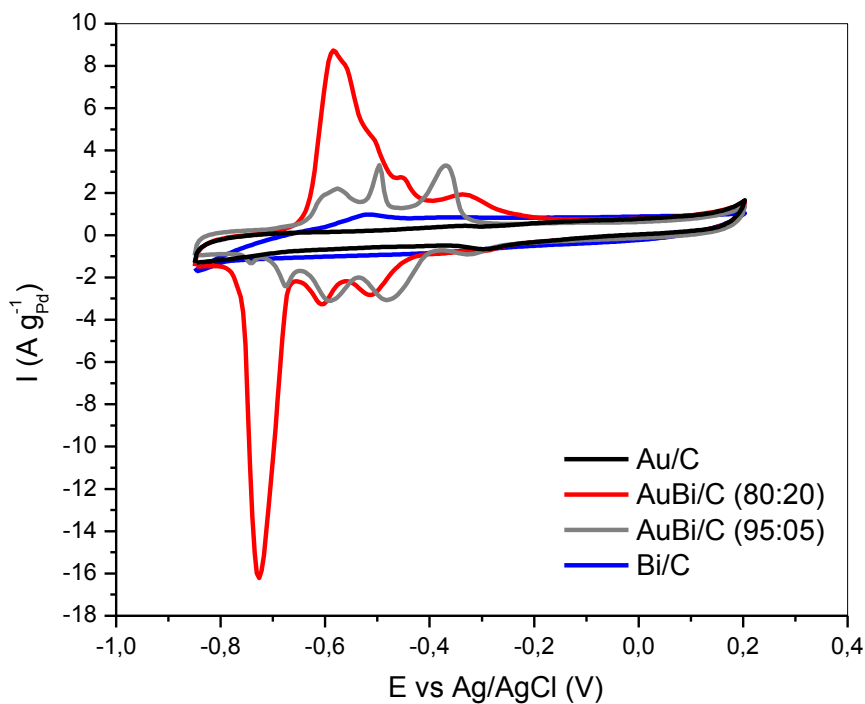
Figure 3. Cyclic voltammograms of Au/C, Bi/C and AuBi/C electrocatalysts in 1.0 mol L^{-1} KOH solution with sweep rate of 10 mV s^{-1}.
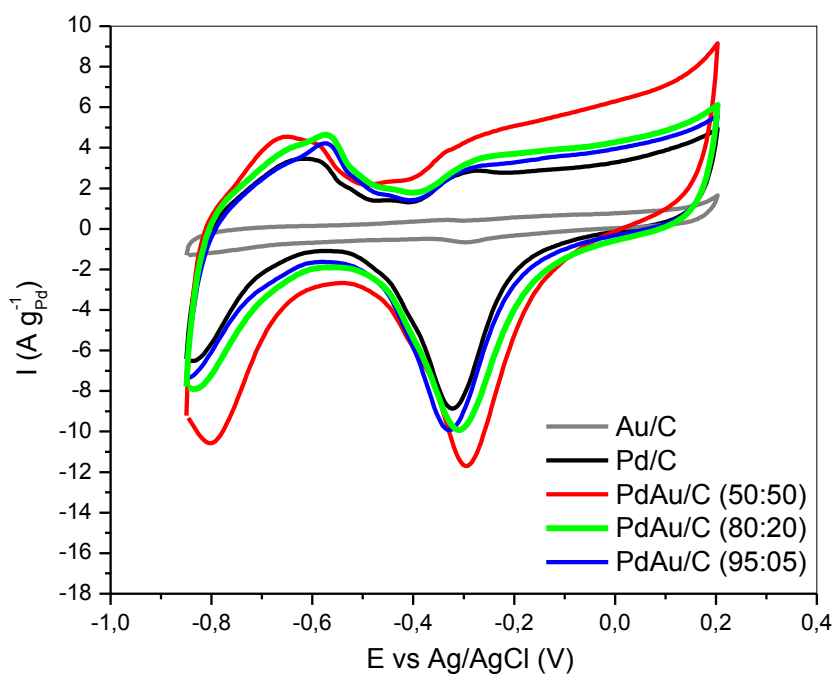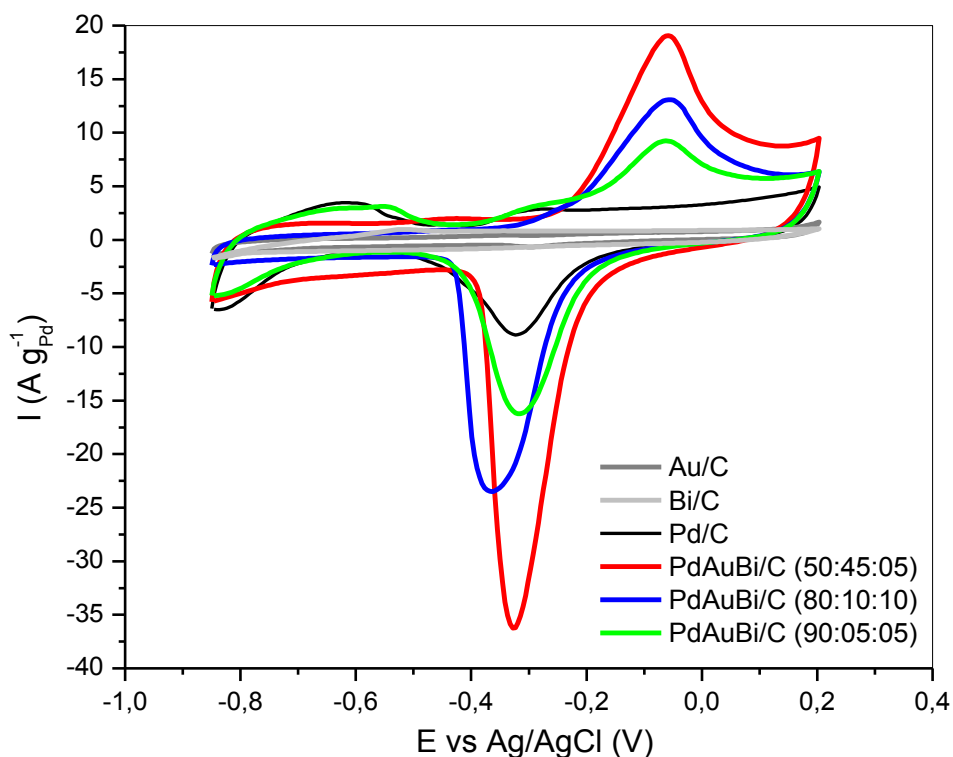

Figure 4. Cyclic voltammograms of Pd/C, Au/C and PdAu/C electrocatalysts in 1.0 mol L^{-1} KOH solution with sweep rate of 10 mV s^{-1}.

The peak at above -0.30 V was attributed to the formation of the Pd(II) oxide layer on the surface of the catalysts [62-64]. Although the mechanism of the oxidation process is not clear, to date, it has been widely accepted that OH$^-$ is first chemisorbed in the initial stage of the oxide formation, and then transformed into higher valence oxides at higher potentials [62]. The adsorption of OH$^-$ starts at the far negative potential from the onset potential of the Pd oxidation and partially overlaps the hydrogen desorption peak, as indicated by peak in the potential range from -0.8 to -0.30 V. Corresponding to the oxidation process, the cathodic peaks, at around -0.3 V, is attributed to the reduction of the Pd(II) oxide during the cathodic scan [62-64]. The voltammetric features of the PdAu/C electrocatalysts were similar to the Pd/C material. However, the clear shifts of the peak positions for the hydrogen adsorption-desorption can be observed in all electrocatalysts indicating the arrangement transformation of Pd atoms as compared with Pd/C; this is in accordance to the observed by others authors [64-67].

Cyclic voltammograms of Pd/C, Au/C, Bi/C and PdAuBi/C electrocatalysts in 1.0 mol L^{-1} KOH solution are shown in Figure 5. PdAuBi/C (50:45:05), PdAuBi/C (80:10:10) and PdAuBi/C (90:05:05) electrocatalysts present a less defined hydrogen adsorption-desorption region compared to PdAu/C (50:50) electrocatalyst. Possibly, the addition of Bi on PdAu/C system leads to the coating of the Pd sites by Bi inhibiting the hydrogen adsorption [16,21,36].


Figure 5. Cyclic voltammograms of Pd/C, Au/C, Bi/C and PdAuBi/C electrocatalysts in 1.0 mol L^{-1} KOH solution with sweep rate of 10 mV s^{-1}.

The peaks located close to -0.1 - 0.0 V were associated to a surface oxidation process [68] and the intensities of these peaks were dependent of Au content. For all PdAuBi/C electrocatalysts the

oxidation current start at -0.2 V which corresponds to the oxidation of the Pd surface in alkaline medium [69,70] according to the reaction:

$$Pd + 2OH^- \rightarrow PdO + H_2O + 2e^-$$

According to the potential-pH diagram of bismuth [71] in aqueous medium, the Bi_2O_3 bismuth oxide phase exists under its hydrated form $Bi(OH)_3$, which is insoluble in alkaline solutions. As referred by the author, bismuth oxidation in aqueous media may start from 0.48 V according to the following reaction:

$$2Bi + 6OH^- \rightarrow 2Bi(OH)_3 + 6e^-$$
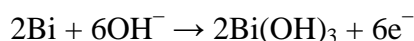
This reaction could be governed by the simultaneous oxidation of the Pd surface. In the negative-going potential scan, a reduction current peak is observable at -0.3 V and was attributed to the reduction of the surface oxides, including bismuth oxides [72] formed during the positive-going potential scan. The potential where the reduction current reaches the maximum absolute value is the same as for the reduction of Pd surface oxide [64,68]. Analogously to the peaks located close to -0.1 - 0.0 V, the intensities of the peaks at about -0.3 V were dependent of Au content indicating the participation of Au species in the process associated to these anodic and cathodic peaks.

The current-time curves of ethylene glycol electro-oxidation on Pd/C, Au/C, AuBi/C, PdAu/C and PdAuBi/C electrocatalysts in 1.0 mol L^{-1} KOH solution are shown in Figure 6a while the final currents obtained in these experiments are presented in Figure 6b.
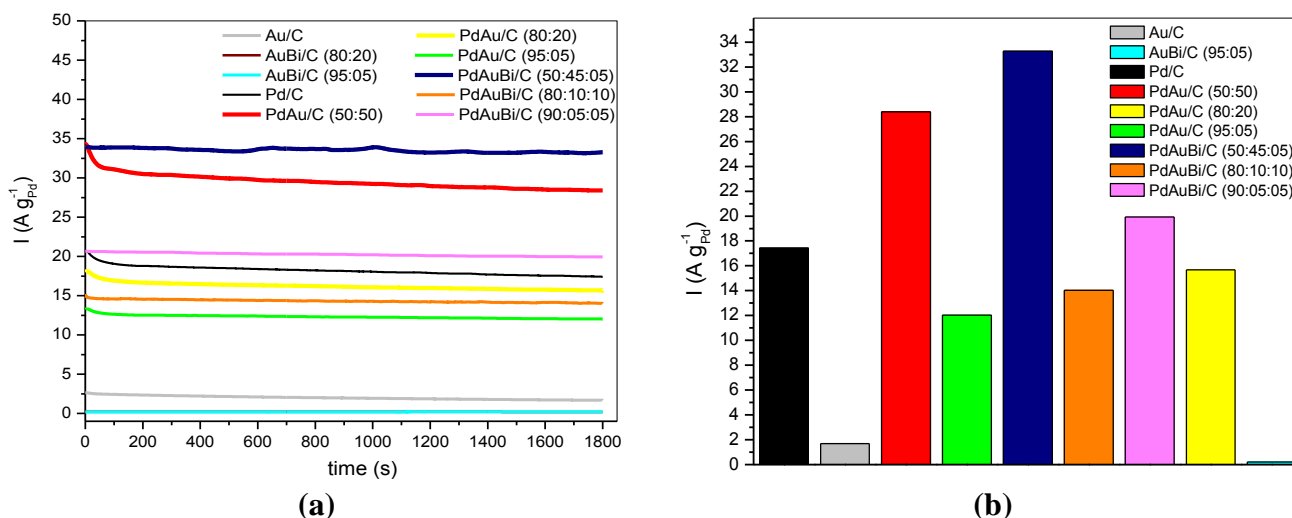
Figure 6. **(a)** Current-time curves of ethylene glycol electro-oxidation on Pd/C, Au/C, AuBi/C, PdAu/C and PdAuBi/C electrocatalysts in 1.0 mol L^{-1} KOH solution after 1800 s at -0.4 V *vs* Ag/AgCl electrode. **(b)** Final currents obtained in chronoamperometry experiments.

The final current values after holding the cell potential at - 0.4 V vs Ag/AgCl for 30 min increase in the following order: PdAuBi/C (50:45:05) > PdAu/C (50:50) > PdAuBi/C (90:05:05) >

Pd/C > PdAu/C (80:20) > PdAuBi/C (80:10:10) > PdAu/C (95:05) > Au/C > AuBi/C (95:05) > AuBi/C (80:20). A comparison between PdAu/C (50:50) and PdAuBi/C (50:45:05) showed a superior electroactivity and stability of the ternary electrocatalyst. This fact indicated a lower deactivation of PdAuBi/C (50:45:05) electrocatalyst probably due to the presence of a greater amount of oxygenated species. The greater amount of oxygenated species can be observed by the higher intensity of the peak at about -0.3 V in the cyclic voltammograms (Fig. 4 and 5). Structural changes in PdAuBi/C electrocatalysts attributed to dissolution and redeposition processes of Bi may also have an important influence in the electroactivity. According to Sieben *et al* [73] the increment of the lattice parameter and the presence of grain boundaries (defects in crystalline lattice) could enhance the adsorption of the alcohols and favor the splitting of the C–C bond leading to an improvement of the electroactivity. Thus, possibly, bifunctional mechanism and structural changes were responsible to the higher performance of PdAuBi/C (50:45:05) electrocatalyst. The addition of small quantities of Bi (5 at.%) to PdAu/C electrocatalyst greatly enhanced the performance for ethylene glycol electro-oxidation in alkaline medium. Recently, Silva *et. al.* [36] evaluated PtAu/C and PtAuBi/C electrocatalysts for methanol and ethanol electro-oxidation in alkaline medium and a significant improvement of activity was also observed for PtAuBi/C catalyst compared to PtAu/C.

4. CONCLUSIONS

The borohydride reduction method was an efficient process to produce of active Pd/C, Au/C, Bi/C, PdAu/C and PdAuBi/C electrocatalysts for ethylene glycol electro-oxidation in alkaline medium. The obtained materials showed the presence of Pd-Au(fcc) alloys, segregated fcc Pd-rich and Au-rich phases and bismuth oxide phases. Electrochemical experiments indicated that the PdAuBi/C (50:45:05) electrocatalyst showed superior activity compared to the others. The addition of small quantities of Bi (5 at.%) to PdAu/C electrocatalyts enhanced the performance for ethylene glycol electro-oxidation in alkaline medium probably due bifunctional mechanism and structural changes in the electrocatalyst.

References

1. M. Linardi, *Introdução à ciência e tecnologia de células a combustível*, Artliber, São Paulo (2010).
2. M.M. Tusi, N.S.O. Polanco, M. Brandalise, O.V. Correa, A.C. Silva, V.A. Ribeiro, A.O. Neto, E.V. Spinacé, *Ionics*, 18 (2012) 215.
3. M.M. Tusi; N.S.O. Polanco, M. Brandalise, O.V. Correa, J.C. Villalba, F.J. Anaissi, A.O. Neto, E.V. Spinacé, *int. J. Electrochem. Sci*., 6 (2011) 484.
4. S. Mekhilef, R. Saidur, A. Safari, *Renew. Sust. Energ Rev.*, 16 (2012) 981.
5. F. Vigier, S. Rousseau, C. Coutanceau, J.M. Léger, C. Lamy, *Top. Catal.*, 40 (2006) 111.
6. P. Zegers, *J Power Sources*, 154 (2006) 497.

7. J.D. Holladay, J. Hu, D.L. King, Y. Wang, *Catal Today,* 139 (2009) 244.
8. M. Balat, *Int. J. Hydrogen Energ*, 33 (2008) 4013.
9. C. Lamy, A. Lima, V. Lerhun, F. Delime, C. Coutanceau, J-M. Léger, *J Power Sources*, 105 (2002) 283.
10. E.V. Spinacé, M. Linardi, A.O. Neto, *Electrochem Commun.*, 7 (2005) 365.
11. J-M. Léger, S. Rousseau, C. Coutanceau, F. Hahn, C. Lamy, *Electrochim Acta*, 50 (2005) 5118.
12. W.J. Zhou, B. Zhou, W.Z. Li, S.Q. Song, G.Q. Sun, Q. Xin, S. Douvartzides, M. Goula, P. Tsiakaras, *J Power Sources*, 126 (2004) 16.
13. H. Liu, C. Song, L. Zhang, J. Zhang, H. Wang, D.P. Wilkinson, *J Power Sources*, 155 (2006) 95.
14. E. Antolini, E.R. Gonzalez, *J Power Sources,* 195 (2010) 3431.
15. S.T. Nguyen, H.M. Law, H.T. Nguyen, N. Kristian, S. Wang, S.H. Chan, X. Wang, *Appl Catal B Environ.*, 91 (2009) 507.
16. A.O. Neto, M.M. Tusi, N.S.O. Polanco, S.G. Silva, M.C. Santos, E.V. Spinacé, *Int. J. Hydrogen Energ.*, 36 (2011) 10522.
17. M.M. Tusi, N.S.O. Polanco, S.G. Silva, E.V. Spinacé, A.O. Neto. *Electrochem Commun.*, 13 (2011) 143.
18. R.M Piasentin, E.V. Spinacé, M.M. Tusi, A.O. Neto, *Int. J. Electrochem. Sci.*, 6 (2011) 2255.
19. J.R. Varcoe, R.C.T. Slade, *Fuel Cells,* 5 (2005) 186.
20. L. Demarconnay, C. Coutanceau, C. Lamy, J.-M. Léger, *J. Power Sources* 156 (2006) 14.
21. L. Demarconnay, S. Brimaud, C. Coutanceau, J-M. Léger, *J. Electroanal. Chem.*, 601 (2007) 169.
22. K. Matsuoka, Y. Iriyama, T. Abe, M. Matsuoka, Z. Ogumi, *J. Power Sources,* 150 (2005) 27.
23. S. Ureta-Zãnartu, C. Yáñez, M. Páez, G. Reyes, *J. Electroanal. Chem.*, 405 (1996) 159.
24. C. Jin, Y. Song, Z. Chen, *Electrochim. Acta*, 54 (2009) 4136.
25. A. Serov, C. Kwak, *Appl Catal B Environ.,* 97 (2010) 1.
26. D. Bayer, S. Berenger, M. Joos, C. Cremers, J. Tubre, *Int. J. Hydrogen Energ.*, 35 (2010) 12660.
27. W. Hauffe, J. Heitbaum, *Electrochim. Acta*, 23 (1978) 299.
28. P.A. Christensen, A. Hamnett, *J. Electroanal Chemistry and Interfacial Electrochem.*, 260 (1989) 347.
29. C. Bianchini, P.K. Shen, *Chem. Rev.*, 109 (2009) 4183.
30. S.Y. Shen, T.S. Zhao, J.B. Xu, Y.S. Li, *J. Power Sources*, 195 (2010) 1001.
31. C. Xu, P.K. Shen, Y. Liu, *J. Power Sources,* 164 (2007) 527.
32. O. Savadogo, K. Lee, K. Oishi, S. Mitsushima, N. Kamiya, K.I. Ota, *Electrochem. Commun.,* 6 (2004) 105.
33. D. Cameron, R. Holliday, D. Thompson, *J. Power Sources*, 118 (2003) 298.
34. C.W. Corti, R.J. Holliday, D.T. Thompson, *Top. Catal.*, 44 (2007) 331.
35. G. Tremiliosi-Filho, E.R. Gonzalez, A.J. Motheo, E.M. Belgsir, J-M. Léger, C. Lamy, *J. Electroanal. Chem.,* 444 (1998) 31.
36. D.F. Silva, A.N. Geraldes, E.Z. Cardoso, M.M. Tusi, M. Linardi, E.V. Spinacé, A.O. Neto, *Int. J. Electrochem. Sci.*, 6 (2011) 3594.
37. J.H. Choi, K.W. Park, I.S. Park, K. Kim, J.S. Lee, Y.E. Sung, *J. Electrochem. Soc.*, 153 (2006) A1812.
38. Y-Z. Su, M-Z. Zhang, X-B. Liu, Z-Y. Li, X-C. Zhu, C-W. Xu, S.P. Jiang, *Int. J. Electrochem. Sci.,* 7 (2012) 4158.
39. E. Casado-Rivera, Z. Gal, A.C.D. Angelo, C. Lind, F.J. DiSalvo, H.D. Abruña, *ChemPhysChem*, 4 (2003) 193.
40. M. Brandalise, M.M. Tusi, R.M. Piasentin, M. Linardi, E.V. Spinacé, A.O. Neto, *Int. J. Electrochem. Sci.*, 5 (2010) 39.
41. E.V. Spinacé, L.A.I. Vale, A.O. Neto, M. Linardi, *ECS Trans.*, 5 (2006) 89.
42. M.-S. Hyun, S-K., Kim, B. Lee, D. Peck, Y. Shul, D. Jung, *Catal Today*, 132 (2008) 138.
43. E.R. Gonzalez, *Quím. Nova*, 23 (2000) 262.

44. E.V. Spinacé, A.O. Neto, M. Linardi, *J. Power Sources*, 129 (2004) 121.
45. C. Xu, L. Cheng, P.K. Shen, Y. Liu, *Electrochem. Commun.*, 9 (2007) 997.
46. Y. Wang, Z.M. Sheng, H. Yang, S.P. Jiang, C.M. Li, *Int. J. Hydrogen Energ.*, 35 (2010) 10087.
47. J.B. Xu, T.S. Zhao, S.Y. Shen, Y.S. Li, *Int. J. Hydrogen Energ.*, 35 (2010) 6490.
48. T.J. Schmidt, Z. Jusys, H.A. Gasteiger, R.J. Behm, U. Endruschat, H. Boennemann,. *J. Electroanal. Chem.*, 501 (2001) 132.
49. W. Juszczyk, Z. Karpinski, D. Lornot, J. Pielaszek, J.W. Sobczak, *J. Catal.*, 151 (1995) 67.
50. J.L. Rousset, J.C. Bertolini, P. Miegge, *Phys. Rev. B*, 53 (1996) 4947.
51. W. Li, *Mater. Chem. Phys.*, 99 (2006) 174.
52. Y. Xiong, M. Wu, J. Ye, Q. Chen, *Mater. Lett.*, 62 (2008) 1165.
53. P. Santhosh, A. Gopalana, K. Lee, *J. Catal.*, 238 (2006) 177.
54. G. Chen, Y. Li, D. Wang, L. Zheng, G. You, C. Zhong, L. Yang, F. Cai, J. Cai, B.H. Chen, *J. Power Sources*, 196 (2011) 8323.
55. C. Rouchowdhry, F. Matsumoto, V.B. Zeldovich, S.C. Warren, P.F. Mutolo, M. Ballesteros, U. Wiesner, H.D. Abruña, F.J. Disalvo, *Chem. Mater.,* 18 (2006) 3365.
56. C. Rouchowdhry, F. Matsumoto, P.F. Mutolo, H.D. Abruña, F.J. Disalvo, *Chem. Mater.*, 17 (2005) 5871.
57. H.T Fan, S.S. Pan, X.M. Teng, C. Ye, G.H. Li, L.D. Zhang, *Thin Solid Films*, 513 (2006) 142.
58. V. Radmilovic, H.A. Gasteiger, P.N. Ross, *J. Catal.*, 154 (1995) 98.
59. L.D. Zhu, T.S. Zhao, J.B. Xu, Z.X. Liang, *J. Power Sources*, 187 (2009) 80.
60. S. M. Skogvold, Ø. Mikkelsen, *Electroanal.*, 20 (2008) 1738.
61. V. Vivier, A. Regis, G. Sagon, J. Y. Nedelec, L. T. Yu, C. Cachet-Vivier, *Electrochim. Acta*, 46 (2001) 907.
62. Z.X. Liang, T.S. Zhao, J.B Xu, *Electrochim. Acta*, 54 (2009) 2203.
63. M. Grden, A. Czerwinski, *J. Solid State Electrochem.*, 12 (2008) 375.
64. J.B. Xu, T.S. Zhao, Y.S. Li, W.W. Yang, *Int J. Hydrogen Energ.*, 35 (2010) 9693.
65. M. Qukaszewski, A. Czerwinski, *Electrochim. Acta*, 48 (2003) 2435.
66. M. Qukaszewski, K. Kusmierczyk, J. Kotowski, H. Siwek, A. Czerwinski, *J Solid State Electrochem.*, 7 (2003) 69.
67. M. Qukaszewski, A. Czerwinski, *J Solid State Electrochem*, 12 (2008) 1589.
68. M. Simões, S. Baranton, C. Coutanceau, *Electrochim. Acta*, 56 (2010) 580.
69. M. Simoes, S. Baranton, C. Coutanceau, *J. Phys. Chem.* C, 113 (2009) 13369.
70. M. Grden, M. Łukaszewski, G. Jerkiewiczb, A. Czerwinski, *Electrochim. Acta,* 53 (2008) 7583.
71. J. Van Muylder, M. Pourbaix, *Atlas d'equilibres electrochimiques a 25 ℃*, Gauthier-Villars & Cie, Paris (1963).
72. I.G. Casella, M. Contursi, *Electrochim. Acta,* 52 (2006) 649.
73. J.M. Sieben, M.M.E. Duarte, *Int. J. Hydrogen Energ.*, 36 (2011) 3313.